Induced Seismicity in the Bergermeer Field: WP1 - Quality Control

Q-con GmbH

Geothermal reservoir engineering

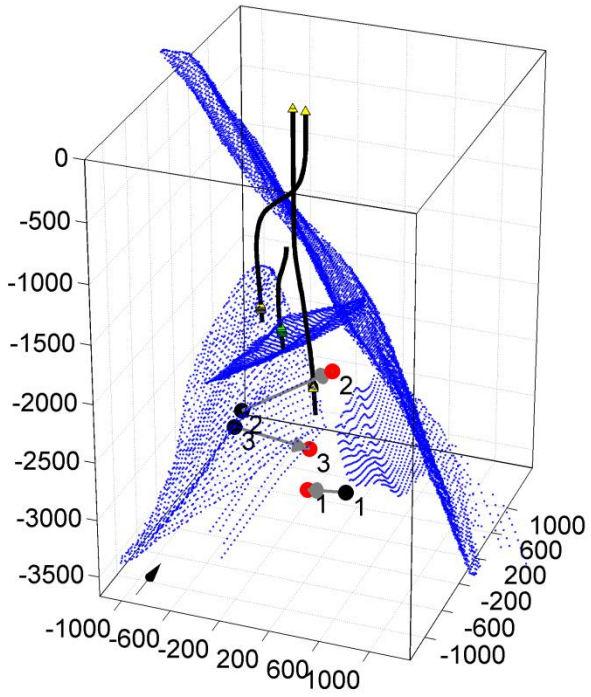

TAQA002

Report title:	Induced Seismicity in the Bergermeer Field: WP1 - Quality Control
Author(s):	Dr. Elmar Rothert; Dr. Robert Vörös; Dr. Stefan Baisch
Report date:	30. November 2015
Project:	Bergermeer
Prepared for:	Taqa Energy B.V.
Version:	151130
Archive No.:	TAQA002

Contents

1 SUMMARY

For a safe operation of the Bergermeer gas storage system, a calibrated geomechanical model is required to forecast the impact of operational activities on induced seismicity. The most important data for calibrating the geomechanical model is the seismicity that occurred previously in the reservoir. For interpreting induced seismicity in the context of the geomechanical model, induced earthquake attributes (i.e. hypocenter location, earthquake strength) need to be determined as accurate as possible, including an estimate of parameter uncertainties.

In the current study we assess the quality of the Bergermeer earthquake data catalogue compiled by different service providers for the time period January 2010 to July 2015.

Seismic monitoring was performed with a 6-level geophone string deployed in existing production wells close to reservoir depth. During the time period under investigation, the geophone string has been re-deployed several times in three different observation wells, BGM6a, BGM3a and BGM5, respectively. In total, 10 phases with different instrument configuration (tool orientations) can be distinguished. At least one calibration shot was fired for each deployment configuration to determine the tool orientations.

Over the time period of more than 5 years, a total number of 380 microearthquakes were recorded. These were assigned magnitudes in the range M_w=-2.9 to M_w=1.1. The strongest earthquake that occurred in the reservoir exhibits M_w=0.7.

Hypocenter locations were provided for all 380 catalogue earthquakes. For these, no event-specific hypocenter location errors were stated. Instead, global (generic) confidence limits were provided for the entire data set, independent of the 10 monitoring phases.

In the current context, we consider the use of generic confidence limits as inappropriate for the following two reasons:

1. The signal-to-noise ratio of checkshot data varies significantly. This implies that the hypocenter location bias associated with the uncertainty of the tool orientations varies significantly for the different phases.
2. The signal-to-noise ratio as well as waveform complexity of reservoir earthquakes varies significantly. A low signal-to-noise ratio as well as a complicated waveform can lead to a false interpretation of phase onsets, implying strong, event-specific variations of hypocenter location errors.

We determined event-specific hypocenter location errors based on the existing catalogue hypocenter locations and the reported tool orientations. For this, we reprocessed raw waveform data to compare observed travel-times and steering vectors with those expected from the reported hypocenter locations. These (event-specific) residuals were then combined with systematic error contributions from uncertainties regarding the seismic wave velocities and the tool orientations. The resulting confidence bounds are considered a realistic estimate of the total hypocenter location error on a 2σ confidence level (i.e. mean location +/- 2σ).

Reprocessing revealed that reported tool orientations are systematically wrong for all phases since January 13th, 2013 during which 157 events occurred. At least for a subset of the data this implies significant hypocenter mislocations. For three events, the hypocenter mislocation was quantified and is in the order of up to 1 km (compare Figure 8). Therefore, we strongly recommend re-processing the entire data set with respect to (Work Package 2, WP2):

- determining tool orientations for all phases,
- determining hypocenter locations for all reservoir events; this should be based on the homogeneous velocity model that was fully calibrated as part of the current study.

We reviewed published event magnitudes. For this, we divided the catalogue into two sets containing earthquakes with hypocentral distances larger, and smaller than 3 km, respectively. For the more distant events (i.e. hypocentral distance > 3 km), event magnitudes cannot be determined reliably due to the large eigenfrequency of the geophones. Associated event magnitudes in the existing catalogue should be interpreted with care as these are subjected to considerable uncertainties.

For reservoir earthquakes (i.e. hypocentral distances ≤ 3 km) we were able to independently reproduce published event magnitude values. Smaller differences were interpreted to result from different model assumptions. As part of WP2, we nevertheless recommend reviewing event magnitudes as changes in hypocenter locations may also affect event magnitudes.

2 DATA BASE SET-UP

Based on the data provisions documented in Appendix A, an earthquake data base was set up for all catalogue events. The data base was built from raw waveform data thus allows reviewing the entire processing chain.

Unless stated otherwise, data processing was performed with Q-con's in house software QUBE 8.0 (e.g. Baisch & McMahon, 2014).

The following processing steps were performed:

a. Earthquake occurrence times and hypocenter locations were assigned according to the earthquake catalogue.

b. SEGY raw data files were extracted for the trigger times of all seismic events as stated in the seismic event catalogue.

c. SEGY raw data files were extracted for the times of calibration shots as stated in the tool orientation reports.

d. The left handed coordinate system of the recording instruments was maintained in the data base.

e. For data conversion to ground velocity, descaling factors as indicated in Table 1 and Table 2 were used. It was confirmed that the descaling factors already account for the gain (email comm. Eric Fortier, MAGNITUDE, November 9th, 2015). Several consistency tests were performed to ensure correct descaling of raw data (e.g. Figure 1).

f. Sensor coordinates and tool orientations were assigned according to the tool orientation reports (A.3).

g. Wellbore trajectories for BGM3a and BGM5 were provided by TAQA.

h. All coordinates were transformed into a local, Cartesian coordinate system centered at the wellhead of BGM3.

i. The sampling frequency of the raw data was obtained from the header information in the SEGY data and the information provided in the MAGNITUDE reports.

surface geophones	
type	SM6, 3 component
resistance	369 Ohm
damping	0.3
eigenfrequency	10 Hz
instrument sensitivity	23.7 V/m/s
gain	12 dB
descaling factor (LSB)	2.935e-7 V/count

Table 1: Acquisition parameters, surface geophones.

downhole geophones	
type	Slimwave, Geospace OMNI-2400, 3 component
resistance	2,400 Ohm
damping	0.57
eigenfrequency	15 Hz
instrument sensitivity	51.59 V/m/s
gain	40 dB
descaling factor (LSB)	3.338e-9 V/count at 1 kHz sample rate 1.335e-8 V/count at 2 kHz sample rate

Table 2: Acquisition parameters, downhole geophones.

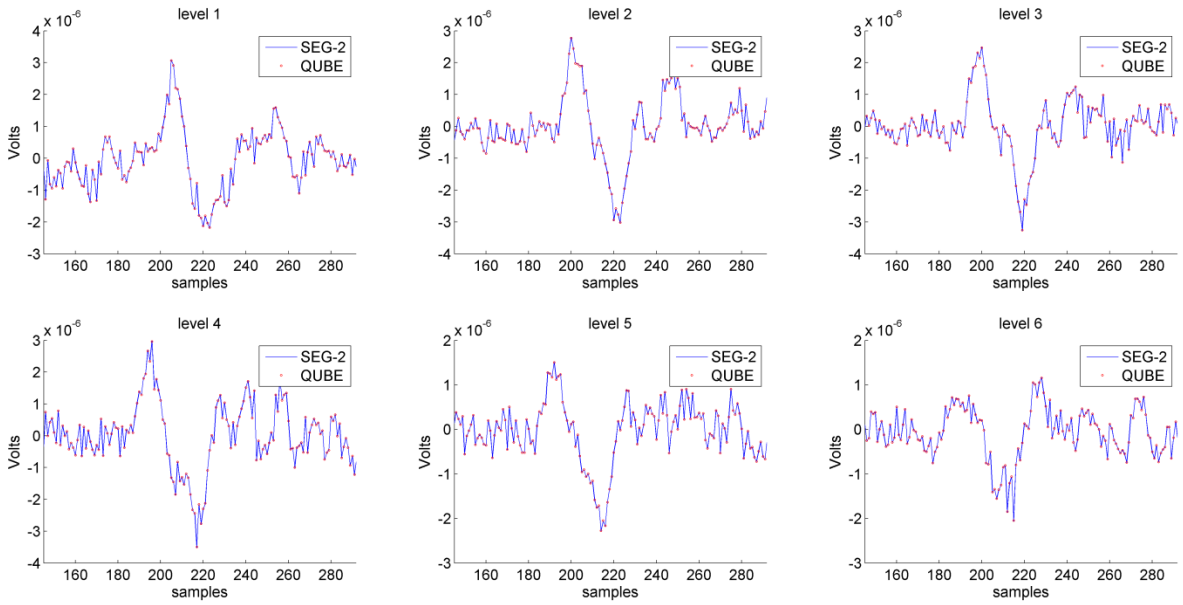

Figure 1: Example waveforms of an event occurring on 14th February 2015, 14:11:54 UTC. Blue line indicates raw data as provided by MAGNITUDE (as event sections stored in SEG-2 data format), red dots refer to seismograms in the QUBE data base. Exact match was confirmed for all traces.

3 BASIC DATA PROCESSING

We determined P- and S-phase onset times for all catalogue events and for 16 checkshots. All phase readings were visually inspected by an experienced seismologist.

Subsequently, we determined the P-phase polarization of all catalogue events using the approach of Jurkevics (1988). For each checkshot and each downhole geophone level, we determined the direction of the incoming signal in 16 time windows with varying length between 0.5 T and 2 T, where T denotes the signal period. We computed the weighted mean from the resulting 16 estimates for azimuth and inclination. Weights are defined as the square of the Jurkevics rectilinearity.

4 REVIEW OF SENSOR ORIENTATIONS

Geophone orientations were provided by MAGNITUDE for all 10 deployment phases (compare tool orientation reports in A.3). These have been determined from checkshots fired at reservoir depth. Table 3 gives an overview of the different deployment phases and the checkshot times. Based on the documents provided, we summarize the orientation procedure applied by MAGNITUDE as follows:

1. sensor orientations were determined by aligning measured checkshot P-wave first motions at each sensor with the theoretical source-station beam direction,
2. the vertical axis of each geophone is assumed to be perfectly aligned with the wellbore trajectory (note: this is the fundamental assumption for obtaining a unique solution to the optimization problem).

In a first step we reviewed reported tool orientations for internal consistency. We note

a. inconsistencies where tabulated rotation angles imply a non-orthogonal coordinate system (MAGNITUDE report 130054, geophone level 6). Associated transformations are physically impossible and we thus interpret the observed inconsistencies as typing errors in the documentation reports. We assume that actual data processing was based on correct tool orientations,
b. false tool orientations reported for phase 8, phase 9, and phase 10. During these phases, the vertical axis of the downhole geophones is not aligned with the wellbore trajectory (Figure 2). This misalignment is also evident when comparing tabulated values for tool orientations with tabulated values of the wellbore trajectory (e.g. MAGNITUDE report 130054). Using these (false) tool orientations for determining hypocenter locations has a first order impact and leads to significant mislocations. Following a Q-con request, false tool orientations for these phases were confirmed by MAGNITUDE (email E. Fortier, MAGNITUDE, November 3rd, 2015),
c. the wellbore trajectories assumed in the tool orientation reports is not always consistent with the wellbore trajectories provided in A.3. We note deviations in the order of ~5 m. We estimate, however, that the error contribution on hypocenter locations resulting from these deviations is much smaller than the overall location error.

Subsequently we reviewed the signal quality of the checkshots to estimate the accuracy to which tools can be oriented. At this stage it is not clear to what extent false tool orientations have been used for determining hypocenter locations. Therefore, our assessment of checkshot quality is conducted in a relative sense, i.e. considering relative precision without accounting for the absolute orientation values.

We used Jurkevics's (1988) method to determine polarization properties by solving the eigenproblem for the covariance matrix of the 3-component seismic signal. The approach

sketched in item 1 of the orientation procedure (see above) is based on the assumption of a linear polarized P-wave. Deviations from linear polarization reduce the accuracy to which the direction of the incoming P-wave can be determined. We used Jurkevics's rectilinearity parameter as a quantitative measure of the degree of linear polarization. For each checkshot and each downhole geophone level, we determined the direction of the incoming signal in 16 time windows with varying length between 0.5 T and 2 T, where T refers to the signal period. We computed the weighted mean from the resulting 16 estimates for azimuth and inclination. Weights are defined as the square of the Jurkevics rectilinearity.

Assuming that misorientations at different geophone levels are independent from each other, we approximate the systematic bias on hypocenter locations by the 2σ confidence interval of the mean misorientation of the 6 geophones (Figure 3). By this we make the simplifying assumption that the hypocenter location procedure can be approximated by a single-station approach performed individually for each downhole geophone. Given the small aperture of the geophone string, we consider this a valid assumption. We note however, that a formal approach will be implemented in WP2 when geophone specific residuals will be projected into the model-space as part of the hypocenter re-location procedure.

Id	Check-shot time	Phase	Document	Well	Operation	Installed
1	17-Jan-2010 13:10:00	test		BGM6(a)		
2	17-Jan-2010 16:06:00		MAG100843			
3	03-Aug-2010 15:32:00	Phase 1	(MAG100553)	BGM3a		
4	03-Aug-2010 18:19:00		MAG100568			
5	05-Nov-2010 12:11:00		MAG100809			5-11-2010
6	22-Mar-2011 13:43:00	Phase 2	MAG110286		Before running up	
7	30-Mar-2011 09:49:00	Phase 3	MAG110315		Running down	30-3-2011
8	30-Mar-2011 12:40:00				Running down	
9	23-Aug-2011 09:39:00		MAG110731 v2		Moved	
10	30-Aug-2011 09:38:00	Phase 4	MAG110751		Running down	30-8-2011
11	24-Jan-2012 11:30:00	Phase 5	MAG120091		Running down	24-1-2012
12	22-May-2012 12:19:00		MAG120482		Moved	
13	31-May-2012 12:28:00	Phase 6	MAG120501		Running down	31-5-2012
14	15-Sep-2012 16:39:00	Phase 7	MAG120831		Running down	14-9-2012
15	15-Jan-2013 16:22:00	Phase 8	MAG130054	BGM5	Running down	13-1-2013
16	25-Jan-2014 10:43:00	Phase 9	MAG140109		Running down	19-1-2014
17	19-Jan-2015 14:11:00	Phase 10	MAG150078	BGM5	Running down	11-1-2015

Table 3: Summary of geophone deployment phases and associated checkshots. Information taken from various reports listed in A.3.

Orientation from shot on 01/15/2013

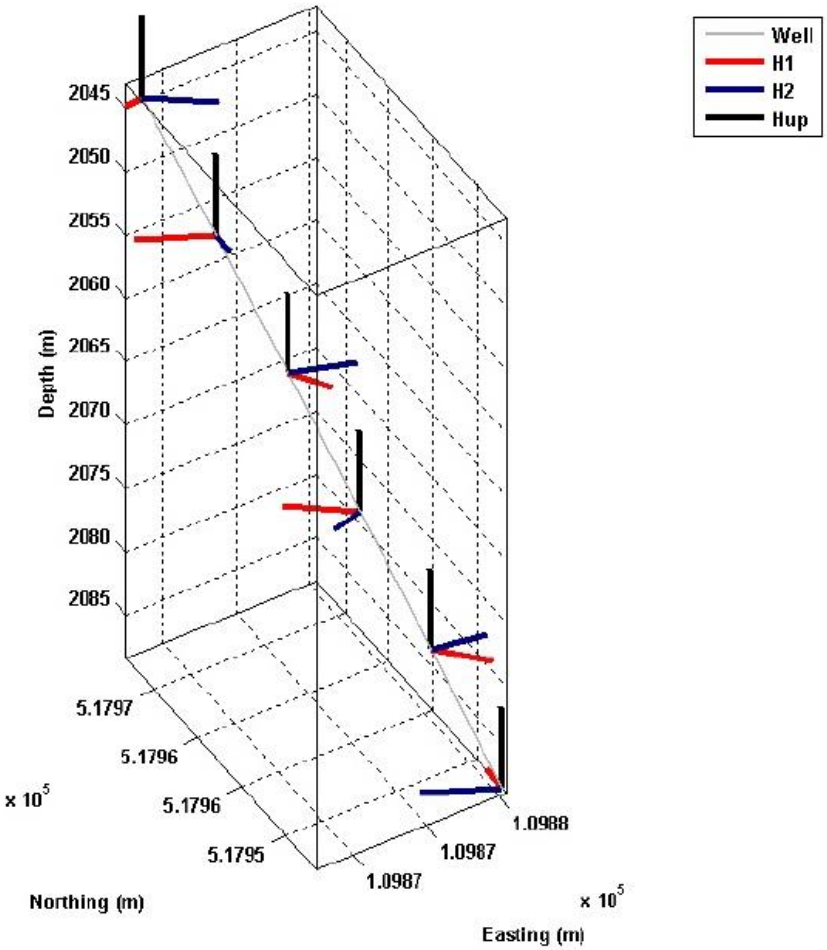

Figure 4: Orientation tools computed from shots performed on 01/15/2013.

Figure 2: Tool orientations reported by MAGNITUDE for Phase 8 (this is Figure 4 from MAGNITUDE report 130054). Sensor orientations for each of the 6 geophone levels are indicated according to the legend. Note: the vertical axis (black) does not align with the wellbore trajectory (grey).

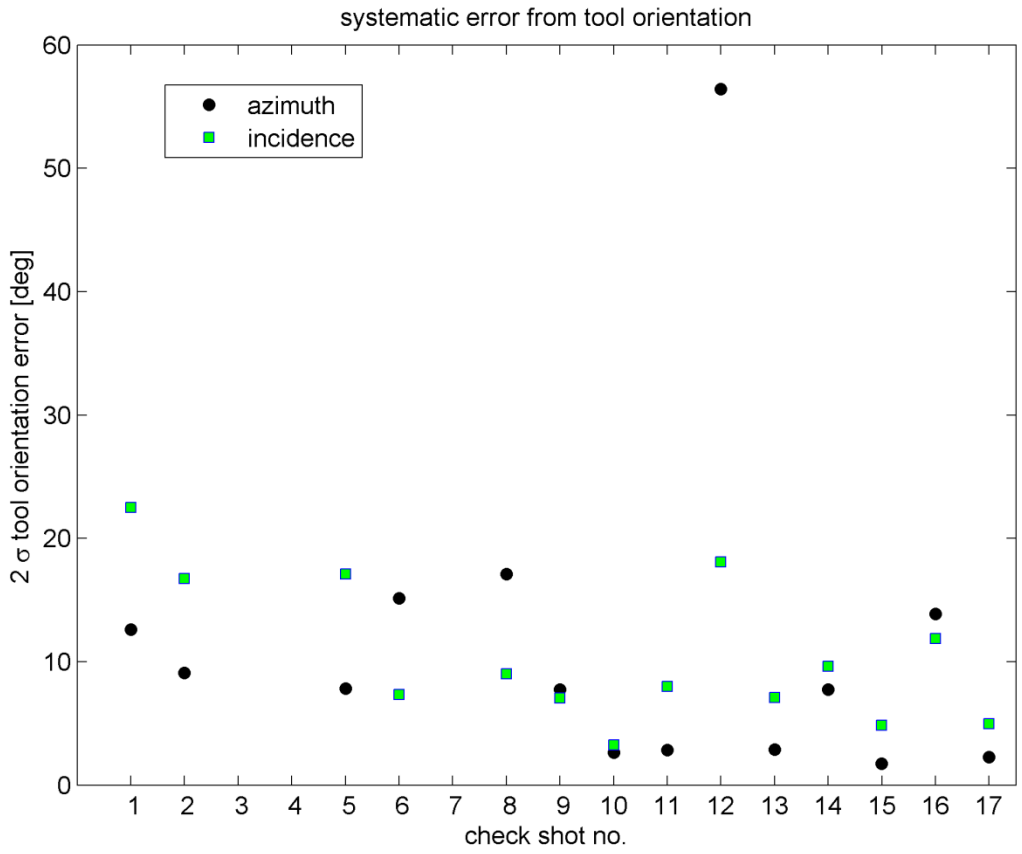

Figure 3: Confidence limits (2σ) for tool orientations determined from different checkshots (Table 3). These confidence limits are an estimator for the systematic hypocenter location bias when using data from all 6 geophones. See text for further details.

5 REVIEW OF SEISMIC VELOCITY MODEL

To assess to what extent hypocenter location estimates are biased by systematic error contributions from seismic velocity model assumptions, we used all checkshot data to calibrate a homogeneous velocity model.

The source times of the checkshots has not been explicitly measured. Thus, P- and S-wave velocities cannot be calibrated individually without additional assumptions. Instead, a combined velocity factor relating S-P differential times to hypocentral distance can be calibrated with the existing data.

Figure 5 shows the resulting velocity model factor for all checkshots for which P- and S-phase onsets could be determined. By averaging over different geophone levels we inherently assume that the seismic velocity model is the same for all ray paths from a given checkshot position to the 6 receiver locations (compare Figure 4). This assumption is clearly justified given the small aperture of the geophone string (50 m) and source-receiver distances of several hundreds of meters.

Although some checkshots with low signal-to-noise ratio exhibit significant scatter, we nevertheless notice that all checkshot data is consistent with the same, homogeneous seismic velocity model. Additionally, the seismic velocity model is well constrained even when accounting for all checkshot data.

For calibrating the seismic velocity model, however, we consider only selected checkshots (id 5, 9, 11, 13, 14 in Table 3) exhibiting the best signal quality. By this, we significantly reduce uncertainties, while the impact on the absolute value of the calibrated model is comparably small (Table 4).

According to the documents provided (A.4) different seismic velocity models have been used for data analysis (Table 4). The KNMI 2 model is consistent with the velocity model calibrated in the current study and we conclude that the 2σ uncertainties obtained in the current study can be applied to the KNMI 2 model.

The homogeneous KNMI 1 model is inconsistent with the checkshot data and for the velocity factor we estimate an uncertainty of +/- 977 m/s (2σ).

Details of the 3D MAGNITUDE model were not investigated, but it was confirmed that the 3D model is not calibrated (phone comm. E. Fortier, November 9th, 2015). Due to the specific receiver geometry, velocity model assumptions have little impact on data residuals and there exists no control on the error contribution from an uncalibrated velocity model. Therefore we recommend not using an uncalibrated 3D model for determining hypocenter locations.

Model	Vp [m/s]	Vs [m/s]	Velocity factor [m/s]	Comment
this study, all checkshots this study, selected checkshots	NA	NA	7,352 +/- 375 7,403 +/- 250	fully calibrated for hypocentral distances up to ~500 m
KNMI 2 (pers. comm. Kraaijpol, November 6th, 2015)	4,655	2,840	7,284	consistent with checkshot data
KNMI 1[1]	4,500	2,700	6,750	inconsistent with checkshot data
MAGNITUDE 3D	variable	1,990[2]	NA	not calibrated

Table 4: Seismic velocity models used for hypocenter determination.

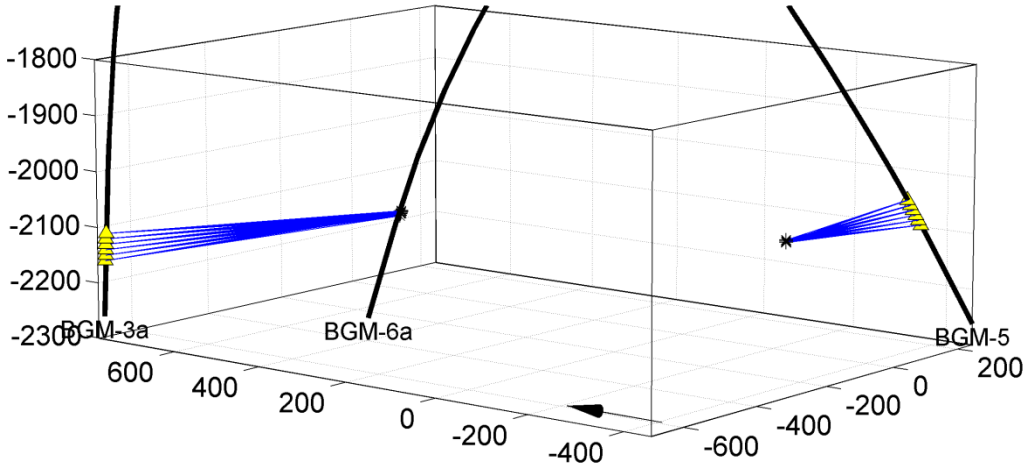

Figure 4: Source-receiver raypaths for the checkshots listed in Table 3. Checkshots which could not be used for calibrating the seismic velocity model are not shown (i.e. checkshot number 1, 2, 3, 4, 7, 12).

[1] Email T.-T. Scherpenhuijsen, October 19th, 2015.
[2] According to MAGNITUDE report 150456 a constant velocity with vs=1,990 m/s has been used.

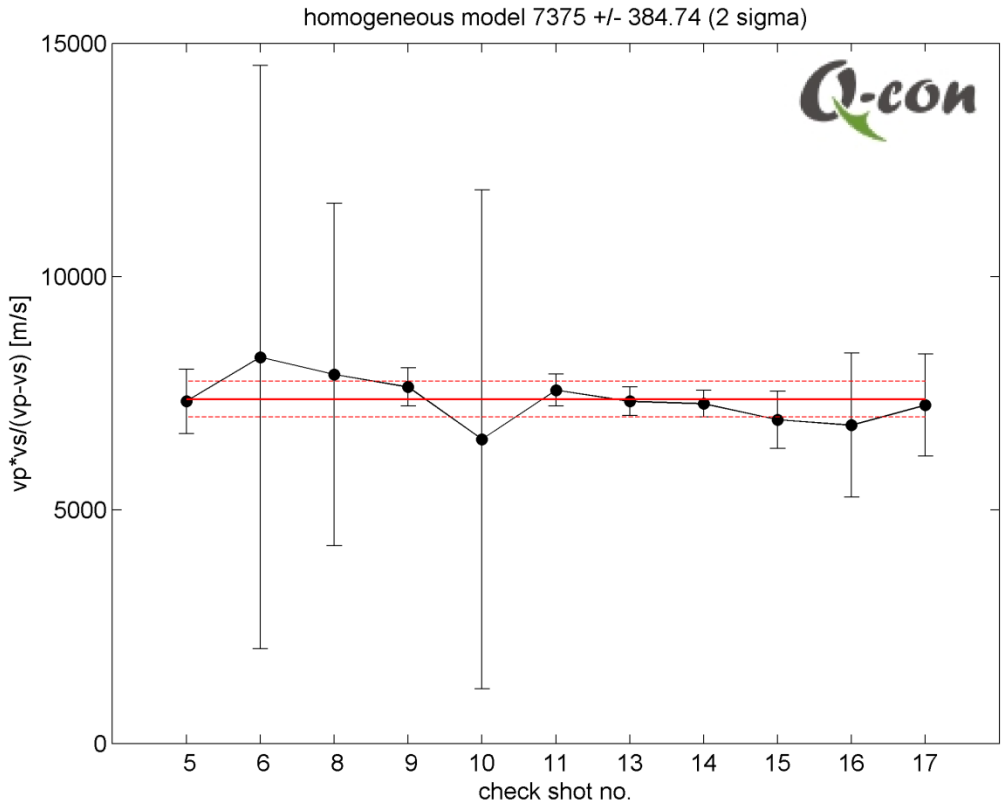

Figure 5: Calibration of the seismic velocity model using checkshots (Table 3) for which P- and S-wave onset times could be identified. Black dots indicate mean velocities per checkshot averaged over the geophone levels. Corresponding errorbars denote the 2σ confidence interval. Large confidence intervals exist for checkshots with low signal-to-noise ratio. All checkshot data is consistent with the averaged, homogeneous model (red line) on a 2σ confidence level.

6 REVIEW OF CATALOGUE HYPOCENTERS

Hypocenter locations were provided for all 380 catalogue earthquakes without stating the event-specific location errors. Instead, event independent confidence limits of

- 20° uncertainty for the azimuthal direction,
- 30° uncertainty for incident,
- 5 ms uncertainty for the timing of the P-wave onset,
- 7.5 ms uncertainty for the timing of the S-wave onset

were stated for the entire data set, independent of the 10 monitoring phases. It is not clear to which confidence level these location uncertainties refer to.

Given considerable variations in signal quality, both for earthquake as well as for checkshot data, we consider the use of generic confidence limits to be inappropriate. Instead, proper error handling should account for the following error contributions:

Systematic error contribution (event independent)		
δV_{mod}	velocity model	determined in chapter 5
δI_{az}	tool orientation, azimuth	determined in chapter 3 for different monitoring phases
δI_{inc}	tool orientation, incident	determined in chapter 3 for different monitoring phases

Table 5: Systematic (event independent) error contributions.

Event specific error contribution		
δSP	“picking errors”	linked to residuals
δAZ	signal direction, azimuth	linked to residuals
δIN	signal direction, incident	linked to residuals

Table 6: Event specific error contributions.

All event specific error contributions (Table 6) are linked to the residuals between model and observation data. These contributions can be directly estimated from the “model fit”. Event independent contributions (Table 5) are not linked to residuals and have to be considered separately, as indicated in Table 5 (last column).

As part of the current study (WP 1), hypocenters were not relocated. Instead, the quality of the existing hypocenter catalogue is assessed based on quantifying the error contributions listed in the tables above.

We determined residuals δSP, δAZ and δIN by comparing observed P-wave directions and differential travel times (chapter 3) to theoretical values associated with catalogue

hypocenter locations. For this, we assumed reported sensor orientations (chapter 4) and the KNMI seismic velocity model (chapter 5).

For a considerable number of events, a symmetrical solution for the hypocenter location (180°-ambiguity in event azimuth) exists due to the specific event-receiver geometry. In the current study we followed the interpretation implicitly stated in the existing hypocenter catalogue, i.e. we determined residuals using the closer of two possible solutions. If hypocenters will be relocated as part of WP2, symmetrical solutions will be reviewed and two alternative solutions may be stated in the re-located catalogue if the symmetry cannot be resolved reliably.

Subsequently, an event-specific location error is determined by combining all error contributions. The resulting confidence bounds (stated in a curvilinear system as azimuth, incidence and distance error) are considered a realistic estimate of the total hypocenter location error on a 2σ confidence level.

We note, however, that the event-specific location errors determined here reflect an approximation resting on several assumptions. Most notably is our assumption that hypocenter locations have been determined using data from all 6 geophones (we have no information about which data has actually been used for determining individual hypocenter locations) and that data uncertainties are independent and Gaussian distributed. Another assumption is that the hypocenter location procedure can be approximated by a single-station approach performed individually for each geophone element. If hypocenters will be relocated as part of WP2, actual residuals will be projected into the model-space. In this case, the approximation sketched above is replaced by a formal approach.

Figure 6 and Figure 7 show the resulting event specific hypocenter location errors. Compared to the generic confidence limits stated for the existing hypocenter catalogue, event specific location errors exhibit significant scatter. In particular, we note time periods where generic confidence limits systematically over predict location errors (e.g. phase 4 in Figure 6), and vice versa (e.g. phase 3 in Figure 6). The latter data example reflects the poor quality of the checkshot data for phase 3.

We note that our assessment of confidence limits is based on the two assumptions that the (mean) catalogue hypocenters are correct and that tool orientations as reported in A.4 were used for processing.

At least one of these assumptions is clearly violated for phases 8, 9, and 10 for which false tool orientations were reported (compare section 4). Figure 8 demonstrates the large impact that false tool orientations have on hypocenter locations. The wrong tool orientations as reported by MAGNITUDE, however, were not used for all events in the hypocenter location procedure. Instead, another set of tool orientations determined by KNMI was used for processing most events in phase 8, 9, and 10. These tool orientations, however, do not account for the 30° inclination of the wellbore thus leading to a systematic bias in hypocenter

locations[3].

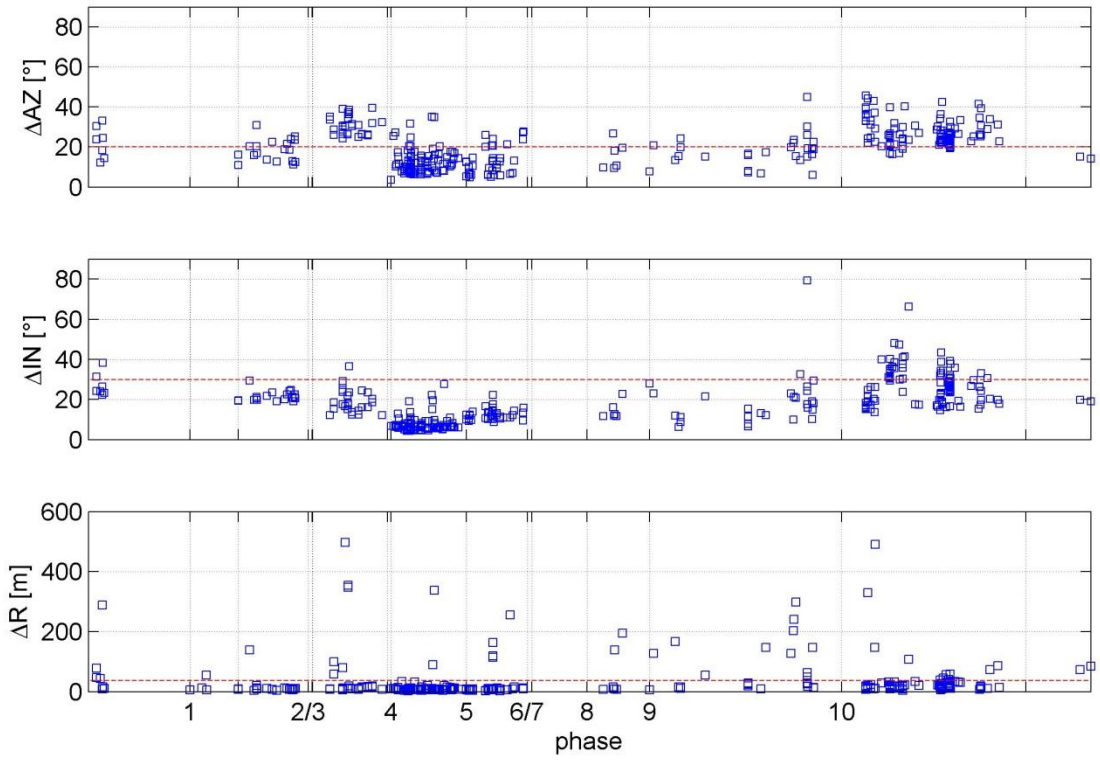

Figure 6: Total uncertainty of hypocenter parameters azimuth, inclination and distance (top to bottom) as a function of time. Time is annotated in terms of the 10 monitoring phases. Generic uncertainties as specified for the existing hypocenter catalogue are denoted by red lines.

[3] email D. Kraaijpool, 10.11.2015

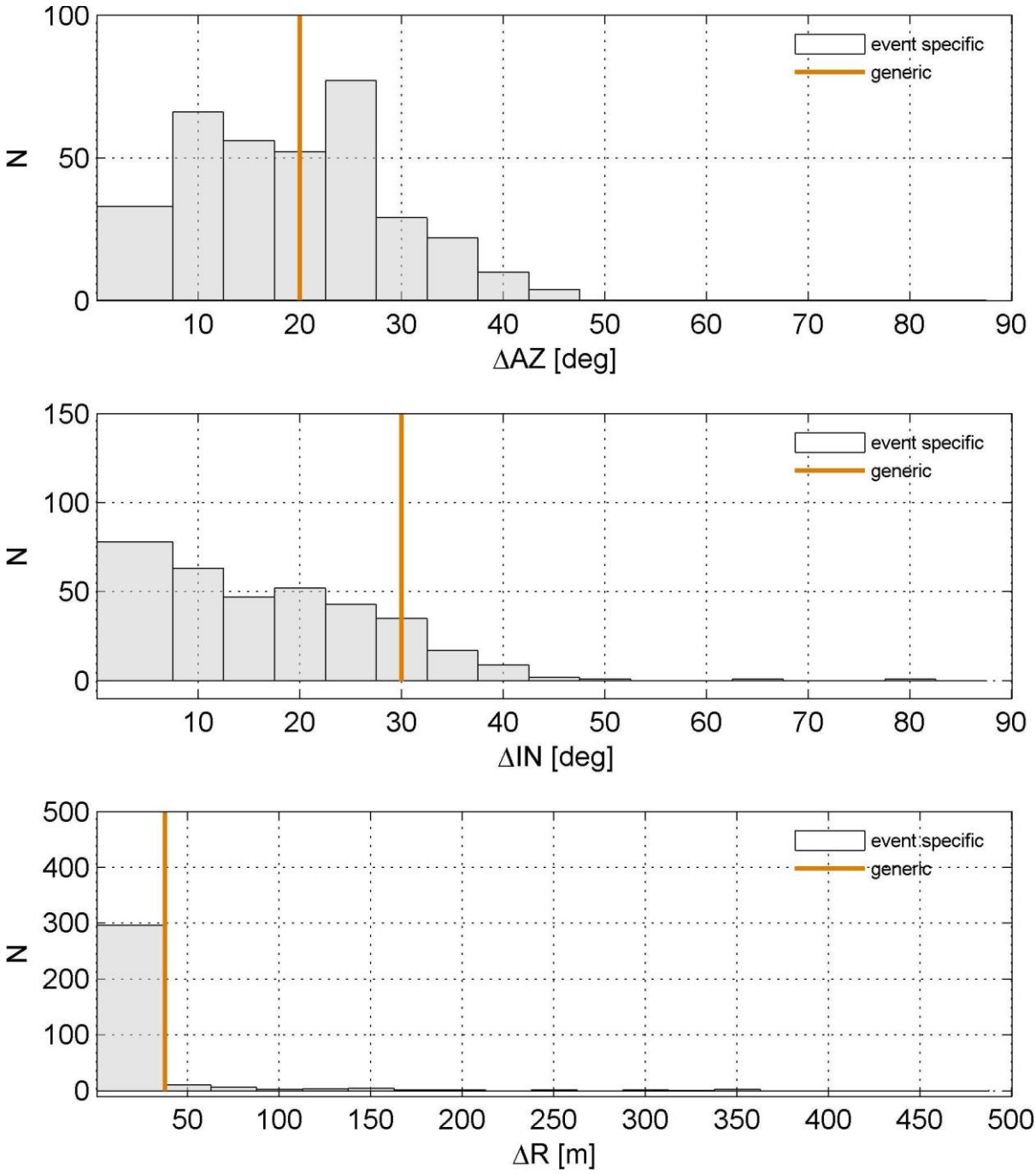

Figure 7: Histograms of event specific hypocenter location errors (from top to bottom: azimuth, incidence, distance) and comparison to generic errors specified for the existing hypocenter catalogue.

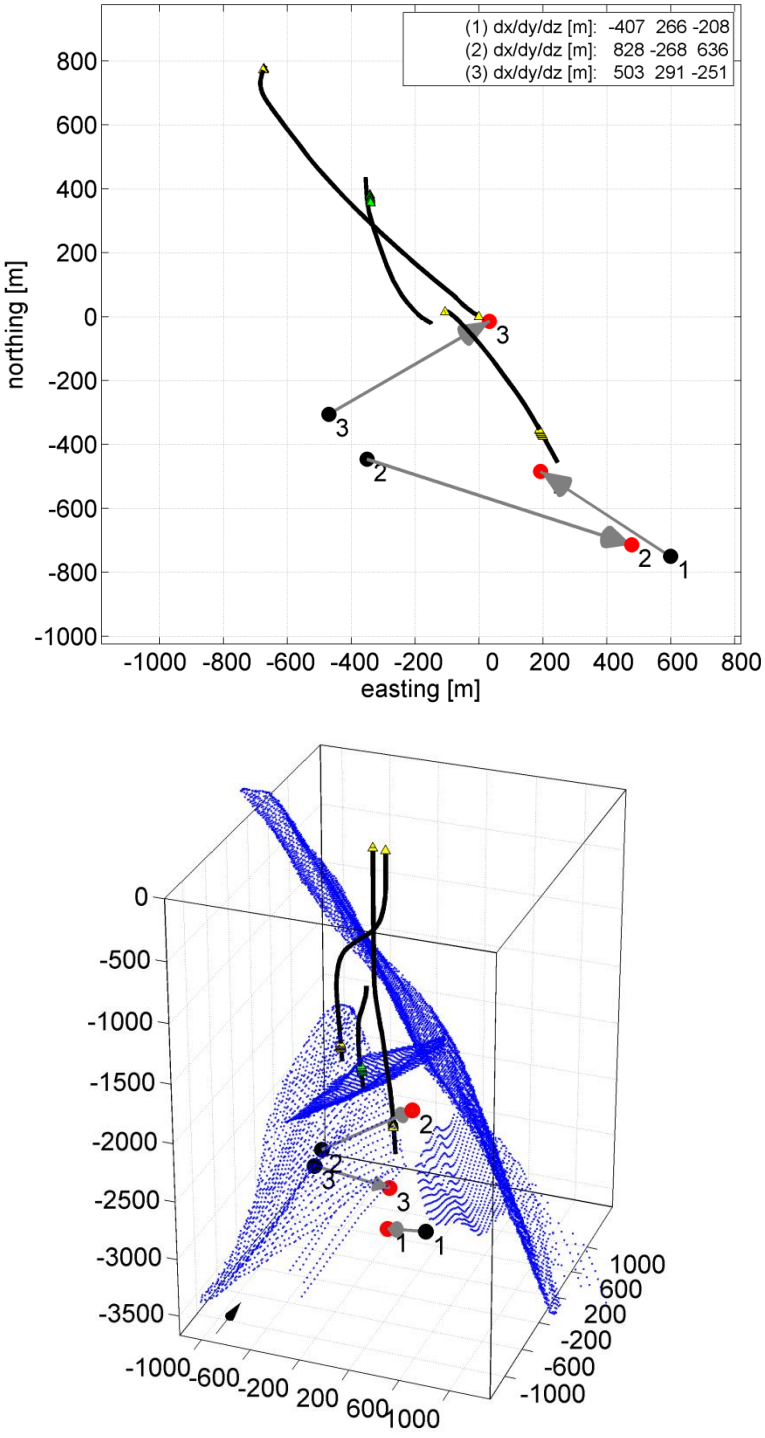

Figure 8: Hypocenter locations of three earthquakes occurring in phase 10 in map view (top) and perspective view (bottom). Black symbol denote hypocenter locations stated in the existing Bergermeer catalogue (i.e. determined using false tool orientations), red symbols denote hypocenter locations for the same events determined with correct tool orientations. Inlet lists relative movements of hypocenter locations (also shown by arrows). Corrected hypocenter locations have been provided by MAGNITUDE (email comm. November 3rd, 2015).

7 REVIEW OF CATALOGUE MAGNITUDES

Different scales exist on which earthquake magnitudes can be expressed. The most common magnitude scales for induced seismicity are local magnitude (M_L) and moment magnitude (M_w). These magnitude scales are both used by the national seismic service (KNMI) to quantify the strength of earthquakes occurring in the Netherlands. KNMI assumes that the two magnitude scales are equivalent in the magnitude range $2.5 < M < 3.5$ (i.e. $M_w \cong M_L$), but is currently reviewing this assumption.

For events in the Bergermeer catalogue, earthquake magnitudes are provided as moment magnitudes (M_w) using the definition of Hanks & Kanamori (1979), which is also used by KNMI. Therefore, the choice of the M_w magnitude scale for Bergermeer seismicity maximizes the consistency with magnitude estimates determined by KNMI. We consider the M_w magnitude as the most appropriate scale for Bergermeer seismicity[4].

The determination of M_w requires several model and parameter assumptions, which are not explicitly stated in the documents provided in A.4. A recent ESG report (A.4) as well as email correspondence with MAGNITUDE indicates that the calculations were based on matching signal spectra by Brune's (1970) ω^2-model.

To investigate consistency and accuracy of the catalogue magnitudes, we re-calculated Hanks & Kanamori (1979) magnitudes using the time-domain approach of Boatwright (1980). Compared to spectral fitting, the time-domain approach requires fewer assumptions and thus is considered more robust in the current context.

Figure 9 compares our magnitude estimates to the existing catalogue magnitudes. Overall, the two magnitude estimates are in reasonably good agreement. Systematic differences exist for the smallest magnitudes, where our estimates are systematically smaller than catalogue magnitudes. We interpret this to (primarily) result from the different assumptions regarding signal attenuation. Without additional calibration data for signal attenuation, no preference for one or the other result can be made.

We consider the difference between the two magnitude estimates shown in Figure 9 to be representative for the general (model dependent) magnitude uncertainty, which is in the order of 0.3 M_w units (1 σ). Furthermore, the largest magnitude event ('Bergen event') exhibits M_w=0.7 on both magnitude scales, consistent with M_w=0.7 reported by KNMI for this event.

We do not show magnitudes determined for events located more than 3 km away from the geophone array. For these, magnitudes cannot be determined reliably due to the large eigenfrequency of the geophones, i.e. the dominating frequencies of the earthquake signals are not properly recorded by the instruments. For the same reason, the geophone array cannot provide reliable magnitude estimates for stronger earthquakes (say M_w>2.0).

[4] We note that the local magnitude scale M_L used by KNMI (Dost et al., 2004) is not calibrated for small magnitude events at hypocentral distances of a few hundred meters only and signals measured at 2 km depth.

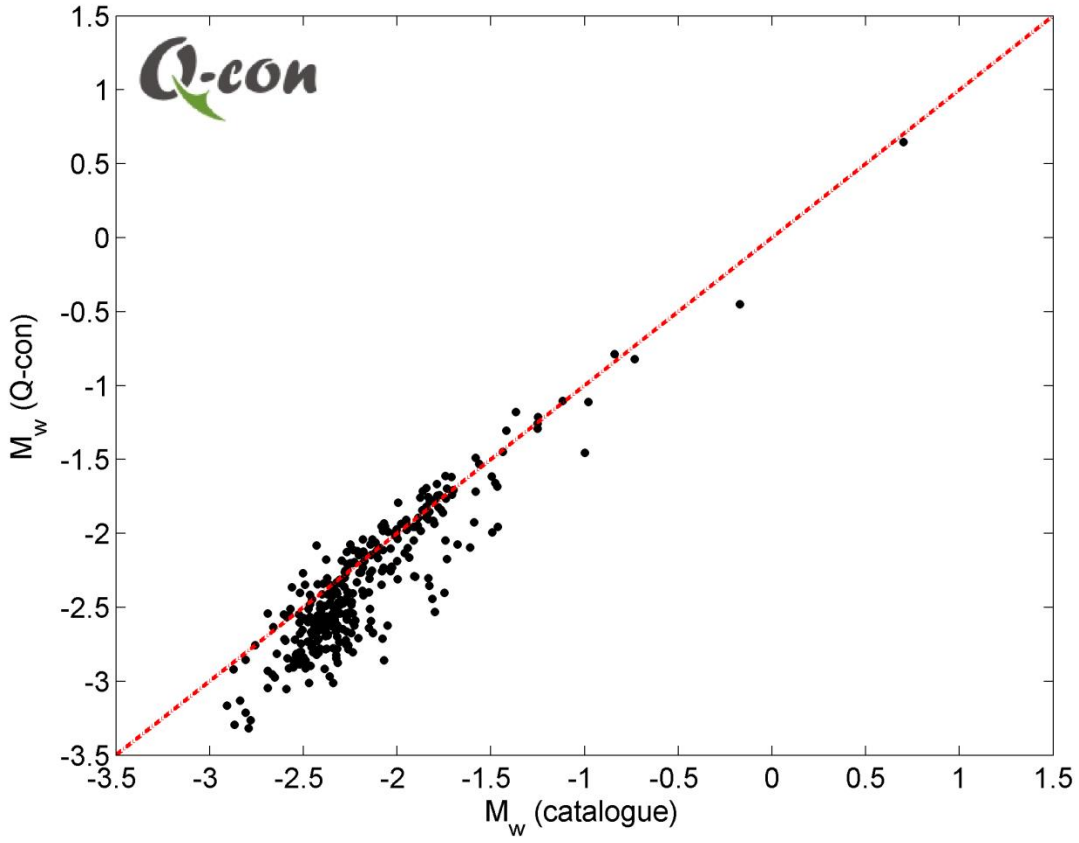

Figure 9: Comparison between catalogue magnitude M_w (catalogue) and M_w (Q-con) determined independently in the current study. Red line denotes equality.

8 REFERENCES

Baisch, S. and A. McMahon, 2014. Seismic Real-Time Monitoring of a Massive Hydraulic Stimulation of a Geothermal Reservoir in the Cooper Basin, Australia. EAGE/DGG Workshop on Microseismic Monitoring, Karlsruhe (Germany). DOI 10.3997/2214-4609.20140005.

Boatwright, J., 1980. A spectral theory for circular seismic sources; simple estimates of source dimension, dynamic stress drop, and radiated energy. *Bull. Seism. Soc. Amer.*, **70**(1), 1-27.

Brune, J., 1970. Tectonic stress and the spectra of seismic shear waves from earthquakes. *J. Geophys. Res.*, **75**, 4997-5009.

Dost, B., Van Eck, T., and H. Haak, 2004. Scaling of peak ground acceleration and peak ground velocity recorded in the Netherlands. *Bol. GeoF. Teo. Appl.*, **45**, 153-168.

Hanks, T. C. and H. Kanamori, 1979. A moment magnitude scale. *J. Geophys. Res.*, **84**, 2348-2350.

Jurkevics, A., 1988. Polarization analysis of three-component array data. *Bull. Seism. Soc. Amer.*, **78**(5), 1725-1743.

APPENDIX A DATA PROVISIONS

Data and documentation were provided on a portable USB disk delivered to Q-con by mail on October, 12th, 2015. The following sections give an overview of the data provided.

A.1. Seismogram Data

- Time continuous seismic raw data for the time period January, 16th 2010 to February 23rd, 2010 and from August 3rd, 2010 to June 4th, 2015. Figure 10 shows the data availability for the entire period of investigation.
- Raw data dayfiles contain 2880 waveform sections of 30 s length. Data is stored in SEGY format with units [counts].
- Waveform sections contain 21 channels (1 surface 3-C geophone, 6 downhole 3-C geophones). The sampling frequency was changed several times throughout the project between 1 kHz and 2 kHz.

Notes on missing data:

- Several dayfiles were incomplete. However, no data is missing during times when catalogue events have occurred.
- No data is available for geophones 5 and 6 in the time period May 22nd to May 31st, 2012 (compared MAG120482).
- No data is available for the check shot on February 9th 2010, 21:03:47 UTC.

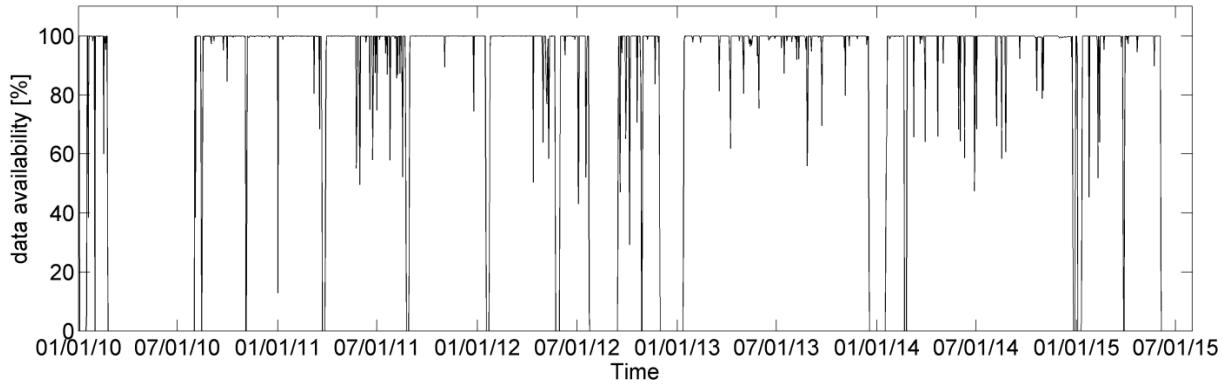

Figure 10: Rawdata availability stated in percent per day as function of time. For the time period January, 16th 2010 to February 23rd, 2010 and August 3rd, 2010 to June 4th, 2015, the average data availability is 88 %.

A.2. Metadata

- A seismic event catalogue was provided containing 380 earthquakes occurring between February 2nd, 2010 and May 25th, 2015 near the Bergermeer field.
- The seismic event catalogue was compiled by KNMI using acquisition settings as reported by MAGNITUDE.
- Between January 2015 and August 2015, MAGNITUDE was in charge of data processing and reporting.
- In July 2015, a new monitoring system was installed, which is currently operated by ESG. No rawdata is available for this time period.

A.3. Additional Data

Document name	Document type
BGM3A_MOD.csv / Copy of BGM3a.csv	Wellbore trajectory BGM3a
Well_BGM5.csv	Wellbore trajectory BGM5

A.4. Documents & Reports

Document name	Document type
Bergermeer6_Monitoring_Field_Report.pdf	Installation report pilot phase
Seismic paperwork_TAQA.xls	Installation report pilot phase
Seismic_Field Report_BGM6a.pdf	Installation report pilot phase
MAG100553.pdf	Installation Report Phase 1
MAG100568_orientation.pdf	Orientation Report Phase 1
MAG100809_orientation.pdf	Orientation Report Phase 1
MAG100843_orientation.pdf	Orientation Report Phase 1
MAG110286 (1).pdf	Orientation Report Phase 2
MAG110286.pdf	Orientation Report Phase 2
MAG110315.pdf	Orientation Report Phase 3
Taqa_MAG110731_v2.pdf	Orientation report Phase 3
Taqa_MAG110751.pdf	Orientation report Phase 4
Taqa_MAG120091.pdf	Orientation report Phase 5
Taqa_MAG120482.pdf	Orientation report Phase 5
Taqa_MAG120501.pdf	Orientation report Phase 6
Taqa_MAG120831.pdf	Orientation report Phase 7
Taqa_MAG130054.pdf	Orientation report Phase 8
Taqa_MAG140109.pdf	Orientation report Phase 9
Taqa_MAG150078.pdf	Orientation report Phase 10
Taqa_MAG100567.pdf	Weekly monitoring report 2010
Taqa_MAG100580.pdf	Weekly monitoring report 2010
Taqa_MAG100603.pdf	Weekly monitoring report 2010
Taqa_MAG100621.pdf	Weekly monitoring report 2010
Taqa_MAG100639.pdf	Weekly monitoring report 2010
Taqa_MAG100659.pdf	Weekly monitoring report 2010
Taqa_MAG100683.pdf	Weekly monitoring report 2010
Taqa_MAG100705.pdf	Weekly monitoring report 2010
Taqa_MAG100742.pdf	Weekly monitoring report 2010
Taqa_MAG100780.pdf	Weekly monitoring report 2010
Taqa_MAG100803.pdf	Weekly monitoring report 2010
Taqa_MAG100832.pdf	Weekly monitoring report 2010
Taqa_MAG100850.pdf	Weekly monitoring report 2010
Taqa_MAG100868.pdf	Weekly monitoring report 2010
Taqa_MAG100896.pdf	Weekly monitoring report 2010
Taqa_MAG100924.pdf	Weekly monitoring report 2010

Appendix A

Document name	Document type
Taqa_MAG100945.pdf	Weekly monitoring report 2010
Taqa_MAG110001.pdf	Weekly monitoring report 2010
Taqa_MAG110051.pdf	Weekly monitoring report 2011
Taqa_MAG110078.pdf	Weekly monitoring report 2011
Taqa_MAG110119.pdf	Weekly monitoring report 2011
Taqa_MAG110137.pdf	Weekly monitoring report 2011
Taqa_MAG110158.pdf	Weekly monitoring report 2011
Taqa_MAG110172.pdf	Weekly monitoring report 2011
Taqa_MAG110200.pdf	Weekly monitoring report 2011
Taqa_MAG110229.pdf	Weekly monitoring report 2011
Taqa_MAG110254.pdf	Weekly monitoring report 2011
Taqa_MAG110285.pdf	Weekly monitoring report 2011
Taqa_MAG110312.pdf	Weekly monitoring report 2011
Taqa_MAG110339.pdf	Weekly monitoring report 2011
Taqa_MAG110373.pdf	Weekly monitoring report 2011
Taqa_MAG110385.pdf	Weekly monitoring report 2011
Taqa_MAG110412.pdf	Weekly monitoring report 2011
Taqa_MAG110438.pdf	Weekly monitoring report 2011
Taqa_MAG110453.pdf	Weekly monitoring report 2011
Taqa_MAG110480.pdf	Weekly monitoring report 2011
Taqa_MAG110487.pdf	Weekly monitoring report 2011
Taqa_MAG110528.pdf	Weekly monitoring report 2011
Taqa_MAG110539.pdf	Weekly monitoring report 2011
Taqa_MAG110559.pdf	Weekly monitoring report 2011
Taqa_MAG110587.pdf	Weekly monitoring report 2011
Taqa_MAG110638.pdf	Weekly monitoring report 2011
Taqa_MAG110653.pdf	Weekly monitoring report 2011
Taqa_MAG110678.pdf	Weekly monitoring report 2011
Taqa_MAG110695.pdf	Weekly monitoring report 2011
Taqa_MAG110714.pdf	Weekly monitoring report 2011
Taqa_MAG110729.pdf	Weekly monitoring report 2011
Taqa_MAG110745.pdf	Weekly monitoring report 2011
Taqa_MAG110773_v2.pdf	Weekly monitoring report 2011
Taqa_MAG110797.pdf	Weekly monitoring report 2011
Taqa_MAG110822.pdf	Weekly monitoring report 2011
Taqa_MAG110840.pdf	Weekly monitoring report 2011
Taqa_MAG110859.pdf	Weekly monitoring report 2011
Taqa_MAG110885.pdf	Weekly monitoring report 2011
Taqa_MAG110923.pdf	Weekly monitoring report 2011

Appendix A

Document name	Document type
Taqa_MAG110942.pdf	Weekly monitoring report 2011
Taqa_MAG110953.pdf	Weekly monitoring report 2011
Taqa_MAG110964.pdf	Weekly monitoring report 2011
Taqa_MAG110994.pdf	Weekly monitoring report 2011
Taqa_MAG111020.pdf	Weekly monitoring report 2011
Taqa_MAG111049.pdf	Weekly monitoring report 2011
Taqa_MAG111070.pdf	Weekly monitoring report 2011
Taqa_MAG111101.pdf	Weekly monitoring report 2011
Taqa_MAG111114.pdf	Weekly monitoring report 2011
Taqa_MAG111137.pdf	Weekly monitoring report 2011
Taqa_MAG120010m.pdf	Weekly monitoring report 2011
Taqa_MAG12038.pdf	Weekly monitoring report 2011
Taqa_MAG120120.pdf	Weekly monitoring report 2012
Taqa_MAG120150.pdf	Weekly monitoring report 2012
Taqa_MAG120189.pdf	Weekly monitoring report 2012
Taqa_MAG120212.pdf	Weekly monitoring report 2012
Taqa_MAG120245.pdf	Weekly monitoring report 2012
Taqa_MAG120260.pdf	Weekly monitoring report 2012
Taqa_MAG120277.pdf	Weekly monitoring report 2012
Taqa_MAG120300.pdf	Weekly monitoring report 2012
Taqa_MAG120323.pdf	Weekly monitoring report 2012
Taqa_MAG120343.pdf	Weekly monitoring report 2012
Taqa_MAG120372.pdf	Weekly monitoring report 2012
Taqa_MAG12038.pdf	Weekly monitoring report 2012
Taqa_MAG120392.pdf	Weekly monitoring report 2012
Taqa_MAG120415.pdf	Weekly monitoring report 2012
Taqa_MAG120430.pdf	Weekly monitoring report 2012
Taqa_MAG120451.pdf	Weekly monitoring report 2012
Taqa_MAG120467.pdf	Weekly monitoring report 2012
Taqa_MAG120484.pdf	Weekly monitoring report 2012
Taqa_MAG120503.pdf	Weekly monitoring report 2012
Taqa_MAG120530.pdf	Weekly monitoring report 2012
Taqa_MAG120546.pdf	Weekly monitoring report 2012
Taqa_MAG12056.pdf	Weekly monitoring report 2012
Taqa_MAG120569.pdf	Weekly monitoring report 2012
Taqa_MAG120590.pdf	Weekly monitoring report 2012
Taqa_MAG120615.pdf	Weekly monitoring report 2012
Taqa_MAG120625.pdf	Weekly monitoring report 2012

Appendix A

Document name	Document type
Taqa_MAG120654.pdf	Weekly monitoring report 2012
Taqa_MAG120675.pdf	Weekly monitoring report 2012
Taqa_MAG120790.pdf	Weekly monitoring report 2012
Taqa_MAG120826.pdf	Weekly monitoring report 2012
Taqa_MAG120846.pdf	Weekly monitoring report 2012
Taqa_MAG120867.pdf	Weekly monitoring report 2012
Taqa_MAG120888.pdf	Weekly monitoring report 2012
Taqa_MAG120913.pdf	Weekly monitoring report 2012
Taqa_MAG120935.pdf	Weekly monitoring report 2012
Taqa_MAG120949.pdf	Weekly monitoring report 2012
Taqa_MAG12098.pdf	Weekly monitoring report 2012
Taqa_MAG121029.pdf	Weekly monitoring report 2012
Taqa_MAG130066.pdf	Weekly monitoring report 2013
Taqa_MAG130093.pdf	Weekly monitoring report 2013
Taqa_MAG130115.pdf	Weekly monitoring report 2013
Taqa_MAG130147.pdf	Weekly monitoring report 2013
Taqa_MAG130174.pdf	Weekly monitoring report 2013
Taqa_MAG130189.pdf	Weekly monitoring report 2013
Taqa_MAG130211.pdf	Weekly monitoring report 2013
Taqa_MAG130247.pdf	Weekly monitoring report 2013
Taqa_MAG130271.pdf	Weekly monitoring report 2013
Taqa_MAG130285.pdf	Weekly monitoring report 2013
Taqa_MAG130316.pdf	Weekly monitoring report 2013
Taqa_MAG130340.pdf	Weekly monitoring report 2013
Taqa_MAG130368.pdf	Weekly monitoring report 2013
Taqa_MAG130382.pdf	Weekly monitoring report 2013
Taqa_MAG130399.pdf	Weekly monitoring report 2013
Taqa_MAG130420.pdf	Weekly monitoring report 2013
Taqa_MAG130440.pdf	Weekly monitoring report 2013
Taqa_MAG130455.pdf	Weekly monitoring report 2013
Taqa_MAG130477.pdf	Weekly monitoring report 2013
Taqa_MAG130501.pdf	Weekly monitoring report 2013
Taqa_MAG130534.pdf	Weekly monitoring report 2013
Taqa_MAG130557.pdf	Weekly monitoring report 2013
Taqa_MAG130579.pdf	Weekly monitoring report 2013
Taqa_MAG130594.pdf	Weekly monitoring report 2013
Taqa_MAG130602.pdf	Weekly monitoring report 2013
Taqa_MAG130618.pdf	Weekly monitoring report 2013

Appendix A

Document name	Document type
Taqa_MAG130644.pdf	Weekly monitoring report 2013
Taqa_MAG130681.pdf	Weekly monitoring report 2013
Taqa_MAG130704.pdf	Weekly monitoring report 2013
Taqa_MAG130725.pdf	Weekly monitoring report 2013
Taqa_MAG130738.pdf	Weekly monitoring report 2013
Taqa_MAG130756.pdf	Weekly monitoring report 2013
Taqa_MAG130773.pdf	Weekly monitoring report 2013
Taqa_MAG130811.pdf	Weekly monitoring report 2013
Taqa_MAG130821.pdf	Weekly monitoring report 2013
Taqa_MAG130845.pdf	Weekly monitoring report 2013
Taqa_MAG130863.pdf	Weekly monitoring report 2013
Taqa_MAG130889.pdf	Weekly monitoring report 2013
Taqa_MAG130934.pdf	Weekly monitoring report 2013
Taqa_MAG130949.pdf	Weekly monitoring report 2013
Taqa_MAG130972.pdf	Weekly monitoring report 2013
Taqa_MAG130997.pdf	Weekly monitoring report 2013
Taqa_MAG131021.pdf	Weekly monitoring report 2013
Taqa_MAG131045.pdf	Weekly monitoring report 2013
Taqa_MAG131080.pdf	Weekly monitoring report 2013
Taqa_MAG131108.pdf	Weekly monitoring report 2013
Taqa_MAG131134.pdf	Weekly monitoring report 2013
Taqa_MAG131160.pdf	Weekly monitoring report 2013
TAQ_MAG130260.pdf	Weekly monitoring report 2014
TAQ_MAG140204.pdf	Weekly monitoring report 2014
TAQ_MAG140239.pdf	Weekly monitoring report 2014
TAQ_MAG140295.pdf	Weekly monitoring report 2014
TAQ_MAG140324.pdf	Weekly monitoring report 2014
TAQ_MAG140346.pdf	Weekly monitoring report 2014
TAQ_MAG140375.pdf	Weekly monitoring report 2014
TAQ_MAG140404.pdf	Weekly monitoring report 2014
TAQ_MAG140443.pdf	Weekly monitoring report 2014
TAQ_MAG140480.pdf	Weekly monitoring report 2014
TAQ_MAG140518.pdf	Weekly monitoring report 2014
TAQ_MAG140549.pdf	Weekly monitoring report 2014
TAQ_MAG140578.pdf	Weekly monitoring report 2014
TAQ_MAG140601.pdf	Weekly monitoring report 2014
TAQ_MAG140631.pdf	Weekly monitoring report 2014
TAQ_MAG140672.pdf	Weekly monitoring report 2014

Appendix A

Document name	Document type
TAQ_MAG140687.pdf	Weekly monitoring report 2014
TAQ_MAG140720.pdf	Weekly monitoring report 2014
TAQ_MAG140732.pdf	Weekly monitoring report 2014
TAQ_MAG140770.pdf	Weekly monitoring report 2014
TAQ_MAG140793.pdf	Weekly monitoring report 2014
TAQ_MAG140823.pdf	Weekly monitoring report 2014
TAQ_MAG140844.pdf	Weekly monitoring report 2014
TAQ_MAG140877.pdf	Weekly monitoring report 2014
TAQ_MAG140912.pdf	Weekly monitoring report 2014
TAQ_MAG140934.pdf	Weekly monitoring report 2014
TAQ_MAG140955.pdf	Weekly monitoring report 2014
TAQ_MAG140978.pdf	Weekly monitoring report 2014
TAQ_MAG141008.pdf	Weekly monitoring report 2014
TAQ_MAG141040.pdf	Weekly monitoring report 2014
TAQ_MAG141063.pdf	Weekly monitoring report 2014
TAQ_MAG141081.pdf	Weekly monitoring report 2014
TAQ_MAG141101.pdf	Weekly monitoring report 2014
TAQ_MAG141135.pdf	Weekly monitoring report 2014
TAQ_MAG141155.pdf	Weekly monitoring report 2014
TAQ_MAG141182.pdf	Weekly monitoring report 2014
TAQ_MAG141207.pdf	Weekly monitoring report 2014
TAQ_MAG141241.pdf	Weekly monitoring report 2014
TAQ_MAG141271.pdf	Weekly monitoring report 2014
TAQ_MAG141295.pdf	Weekly monitoring report 2014
TAQ_MAG141318.pdf	Weekly monitoring report 2014
TAQ_MAG141350.pdf	Weekly monitoring report 2014
TAQ_MAG141376.pdf	Weekly monitoring report 2014
TAQ_MAG141402.pdf	Weekly monitoring report 2014
TAQ_MAG141419.pdf	Weekly monitoring report 2014
Taqa_MAG140081.pdf	Weekly monitoring report 2014
Taqa_MAG140111.pdf	Weekly monitoring report 2014
Taqa_MAG140140.pdf	Weekly monitoring report 2014
Taqa_MAG140169.pdf	Weekly monitoring report 2014
TAQ_MAG150010.pdf	Weekly monitoring report 2015
TAQ_MAG150053.pdf	Weekly monitoring report 2015
TAQ_MAG150074.pdf	Weekly monitoring report 2015
TAQ_MAG150105.pdf	Weekly monitoring report 2015
TAQ_MAG150138.pdf	Weekly monitoring report 2015

Appendix A

Document name	Document type
TAQ_MAG150168.pdf	Weekly monitoring report 2015
TAQ_MAG150190.pdf	Weekly monitoring report 2015
TAQ_MAG150210.pdf	Weekly monitoring report 2015
TAQ_MAG150242.pdf	Weekly monitoring report 2015
TAQ_MAG150265.pdf	Weekly monitoring report 2015
TAQ_MAG150280.pdf	Weekly monitoring report 2015
TAQ_MAG150296.pdf	Weekly monitoring report 2015
TAQ_MAG150312.pdf	Weekly monitoring report 2015
TAQ_MAG150334.pdf	Weekly monitoring report 2015
TAQ_MAG150352.pdf	Weekly monitoring report 2015
TAQ_MAG150367.pdf	Weekly monitoring report 2015
TAQ_MAG150383.pdf	Weekly monitoring report 2015
TAQ_MAG150397.pdf	Weekly monitoring report 2015
TAQ_MAG150411.pdf	Weekly monitoring report 2015
TAQ_MAG150422.pdf	Weekly monitoring report 2015
TAQ_MAG150430.pdf	Weekly monitoring report 2015
TAQ_MAG150437.pdf	Weekly monitoring report 2015
TAQ_MAG150454.pdf	Weekly monitoring report 2015
TAQA_MAG150303.pdf	Monthly monitoring report 2015
TAQA_MAG150456.pdf	Monthly monitoring report 2015
TAQA Bergermeer - August, 2015 Monthly Report.pptx	Monthly monitoring report ESG 2015
TAQA Bergermeer - September, 2015 Monthly Report.pptx	Monthly monitoring report ESG 2015